Process-dependent thermal transport properties of silicon-dioxide films deposited using low-pressure chemical vapor deposition

Y. S. Ju and K. E. Goodson[a)]
Department of Mechanical Engineering, Stanford University, Stanford, California 94305-3030

(Received 19 October 1998; accepted for publication 2 February 1999)

The volumetric heat capacity and thermal conductivity of silicon-dioxide films prepared using low-pressure chemical vapor deposition (LPCVD) are measured. The measurements employ the 3ω technique, which is extended to determine the thermal conductivity anisotropy and volumetric heat capacity of thin dielectric films. The thermal conductivity of the silicon-dioxide films exhibits a significant process dependence, which cannot be attributed to highly oriented microvoids or impurities. The volumetric heat capacity, in contrast, is largely independent of processing history provided that appropriate corrections are made to account for porosity and impurity contributions. This study provides evidence that process-dependent structural disorder strongly influences the thermal conductivity of amorphous films. © *1999 American Institute of Physics.* [S0021-8979(99)01110-X]

I. INTRODUCTION

Advances in a growing number of electrical and optical devices and systems rely on the proper understanding of heat transport in thin dielectric films. The damage threshold of mirrors and coatings is often determined by thermal properties of the constituent dielectric films.[1,2] Heat conduction through dielectric passivation layers in integrated circuits has a strong influence on the reliability of interconnects and transistors.[3] The rate of heat removal dictates the operation bandwidth of data storage devices based on thermally-induced phase transition phenomena.

The majority of thin dielectric films are deposited at relatively low temperatures leading to microstructures and compositions very different from those in bulk materials. The possible influence of these differences on thermal transport properties is of significance, not only to the optimization of process conditions, but also to the fundamental understanding of heat transport in dielectric materials.

In a series of articles,[4–7] Cahill and co-workers investigated the out-of-plane thermal conductivities of silicon-dioxide films prepared using different methods. Reduction by as much as 50% from the value of bulk fused silica was observed. Measurements were also performed for silicon-dioxide films deposited using low-pressure chemical vapor deposition (LPCVD).[8] High-temperature annealing caused the thermal conductivity to approach that of thermally grown silicon-dioxide films. A more recent study on LPCVD and plasma enhanced chemical vapor deposition silicon-dioxide films yielded results that are consistent with the previous data.[9] Figure 1 plots existing data on those silicon-dioxide films for which density data are also available. Shown as a dotted line is the prediction of the effective medium theory, where the density deficit and thermal conductivity reduction are modeled using spherical microvoids uniformly distributed within a fully dense silicon-dioxide matrix. The thermal conductivity of the effective medium k is given by[10]

$$4k=(3f_1-1)k_1+(3f_2-1)k_2 + \{[(3f_1-1)k_1+(3f_2-1)k_2]^2+8k_1k_2\}^{1/2}, \quad (1)$$

where k_1 is the thermal conductivity of the silicon-dioxide matrix, k_2 is the thermal conductivity of air that is assumed to fill the microvoids, and f_1 and f_2 are the volume fractions of the matrix and microvoids, respectively. The contribution to heat conduction by the air in the microvoids is appreciable only for highly porous films. In contrast to the case of Vycor,[11] which is bulk porous glass, the reduction in the thermal conductivities of the silicon-dioxide films cannot be accounted for by the consideration of porosity alone. Measured thermal conductivities of amorphous carbon and diamond-like-carbon films[12] also revealed that deposition conditions considerably affect the film thermal conductivity.

The present study reports measurements of the volumetric heat capacity and anisotropy in the thermal conductivity of silicon-dioxide films prepared using the thermal oxidation and LPCVD processes. Simultaneous measurements of the heat capacity and thermal conductivity provide further information about the nature of the observed thermal conductivity reduction. This work examines the possibility that highly oriented microvoids are responsible for reduction in the out-of-plane thermal conductivity. The experimental data are discussed in connection with existing structural analyses of chemical vapor deposition (CVD) silicon-dioxide films previous theoretical studies on heat conduction mechanisms in amorphous materials.

II. EXPERIMENTS

A. Sample preparation

Seven different types of silicon-dioxide samples are prepared using thermal oxidation and LPCVD. The LPCVD silicon-dioxide films are deposited at 300 and 400 °C using silane as a silicon source. One set of the films is doped with

a)Electronic mail: goodson@vk.stanford.edu

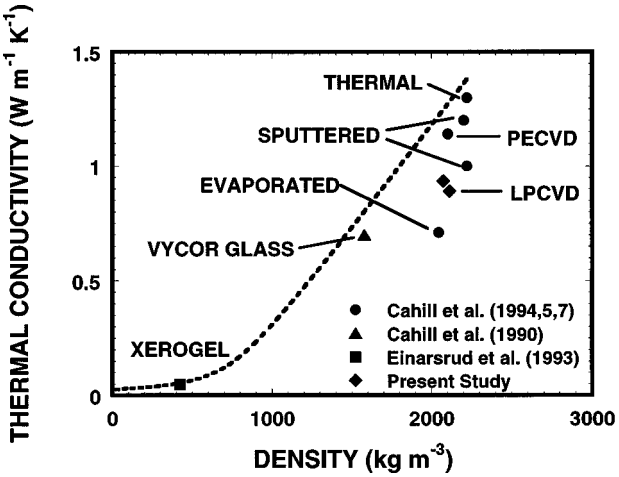

FIG. 1. Measured out-of-plane thermal conductivities of silicon-dioxide layers prepared using different methods (see Refs. 4–7). The LPCVD data are from the present study. The data of porous silica glass (see Ref. 11) and xerogel (see Ref. 28) are included for comparison. The dotted line is the prediction of the effective medium theory.

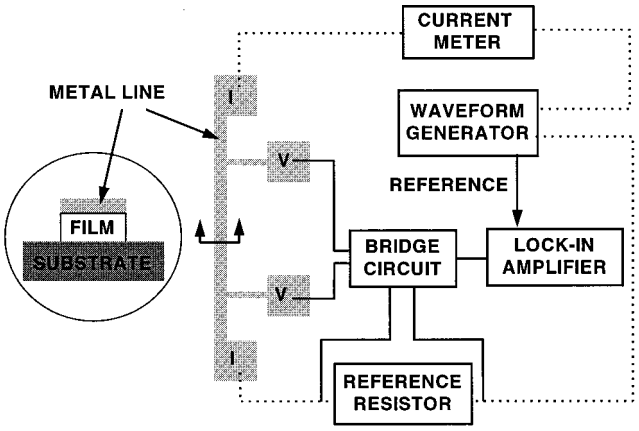

FIG. 2. Experimental setup for the thermal property measurement technique described here. The lock-in amplifier is equipped with a frequency tripler. Details of the bridge circuit are available in the literature (see Ref. 13).

phosphorus at a concentration of 7% by introducing PH_3 during the deposition. Half of the deposited films are annealed at 900 °C for 45 min. Wet thermal oxidation at 900 and 1100 °C yields the thermally-grown silicon-dioxide film. Aluminum layers are sputtered on the silicon-dioxide films and patterned lithographically through wet etching. Prior to each film deposition, the wafers are treated using the standard diffusion clean process (10 min in 4:1 sulfuric-acid and hydrogen-peroxide solution, 10 min in 5:1:1 deionized water, hydrochloric-acid, and hydrogen-peroxide solution, 30 s HF dip). The thicknesses of the silicon-dioxide films, which range between 0.1 and 2 μm, are measured using an ellipsometer and a laser interferometer. A surface profilometer measures the thickness of the aluminum films to be around 0.25 μm.

To help interpret the heat capacity data and also to obtain film density, Fourier transform infrared (FTIR) and rutherford back scattering/hydrogen forward scattering (RBS/HFS) analyses are conducted. The infrared absorption spectra are analyzed to obtain the relative number densities of hydrogen atoms present in the film in the form of water, hydroxyl ions or Si–H. Combined RBS/HFS analysis probes both forward and backward scattered helium atoms and yields absolute atom concentrations. The maximum probe depth of the HFS technique is limited to approximately 500 nm due to the large incident angle of the helium ion beam. Hydrogen concentrations at locations beyond the probe limit are assumed to be constant at a value prevailing within the probe volume. The depth profiles acquired up to 500 nm exhibit no appreciable concentration gradients for all the films investigated.

B. Thermal conductivity and heat capacity measurements

The 3ω technique[4,13] has been adapted to perform simultaneous measurements of the thermal conductivity k_f and volumetric heat capacity C_f of a thin dielectric film. In this technique harmonic Joule heating is induced in a metal line deposited on a dielectric film using a waveform generator. The resulting temperature oscillations at twice the current frequency are extracted by monitoring the third harmonic component of the voltage drop across the metal line using a bridge circuit and a lock-in amplifier. A detailed description of the procedure required to measure the 3ω voltage has been reported elsewhere[13] and will not be repeated here. A schematic diagram of the metal bridge structure and experimental setup used in the present study is shown in Fig. 2.

The temperature rise in the metal exhibits a frequency dependence that is governed by the thermal properties of the dielectric film. At frequencies much lower than the thermal diffusion frequency of the film, $k_f/C_f d_f^2$, the component of the steady-periodic temperature oscillations that is in phase with the harmonic heating consists of two contributions: One from the film, ΔT_f, and the other from the substrate, ΔT_{sub}. The temperature rise ΔT_f is inversely proportional to the film thermal conductivity but is independent of the film heat capacity. At very high frequencies, in contrast, the substrate contribution becomes negligible and the temperature rise in the metal depends on the heat capacity, as well as thermal conductivity of the dielectric film. With the thermal conductivity determined from the low-frequency data, the heat capacity is obtained by comparing the high-frequency data with solutions to the heat diffusion equation.

An analytic expression was derived for the in-phase component of temperature oscillations at frequencies much lower than the heat diffusion frequency of the dielectric film.[7] The substrate contribution ΔT_{sub} varies logarithmically with the heating frequency while the film contribution is frequency independent and given by

$$\Delta T_f = \Psi \frac{P'}{w} \frac{d_f}{k_f}. \tag{2}$$

Here w is the width of the metal line and P' is the amplitude of power dissipation per unit length of the metal line. The factor Ψ accounts for heat spreading within the film and is a function of the ratio between the in-plane and out-plane thermal conductivities and the film thickness.[14] In the experi-

ments, the film contribution to the temperature rise ΔT_f is obtained by subtracting ΔT_{sub} from the measured amplitude of total temperature oscillations. Data analysis can be greatly simplified by using a quasi-one-dimensional structure ($\Psi = 1$), which enables the out-of-plane thermal conductivity to be determined independent of the in-plane thermal conductivity. A mesa structure depicted in Fig. 2 or a structure with the ratio w/d_f much larger than unity are examples of a quasi-one-dimensional structure.

A solution applicable at high heating frequencies can be derived for a quasi-one-dimensional structure when the following simplifying assumptions are made: (1) The temperature rise in the substrate can be neglected compared with that in the metal line. (2) The metal line is isothermal. (3) Direct heat loss to the ambient from the metal and dielectric films is negligible. The amplitude of the in-phase component of temperature oscillations in the metal line is then given as the real part of

$$\Delta \tilde{T}_m = \frac{P'}{w} \frac{(d_f/k_f)(\tanh \beta/\beta)}{1 + i2\pi f_h C_m d_m (d_f/k_f)(\tanh \beta/\beta)}. \quad (3)$$

Here β is a complex number representing the ratio of the film thickness to the thermal diffusion length, $d_f(i2\pi f_h C_f/k_f)^{1/2}$. The earlier analytic solution agrees well with numerical solutions to the heat equation for the films studied here. Note that the temperature rise in the metal line depends also on the volumetric heat capacity C_m and thickness d_m of the metal layer. Thick metal films obscure the influence of the film heat capacity on ΔT_m and degrade the accuracy.[15] To achieve adequate accuracy, it is also important to require that the film thickness be close to or greater than the heat diffusion length at the maximum heating frequency, which is given as $(k_f/2\pi C_f f_{h,\max})^{1/2}$. The maximum heating frequency in the present study is 65 kHz, which is dictated by the bandwidth limit of the lock-in amplifier used. The use of a high temporal resolution thermometry technique, such as the thermoreflectance technique,[3] in conjunction with a high-frequency lock-in amplifier will enable measurements on thinner films.

Figure 3 shows the measured frequency dependence of the amplitude of temperature oscillations for the case of the silicon-dioxide film grown at 900 °C. The thermal conductivity of the substrate, which is needed to compute the substrate contribution to temperature rises ΔT_{sub}, is deduced independently using the original 3ω method.[13] The dotted line represents the amplitude of temperature oscillations calculated using Eq. (3), which neglects the substrate temperature rise. The enlarged view of the high-frequency region is shown as an inset in Fig. 3 along with predictions using three different values for the film heat capacity.

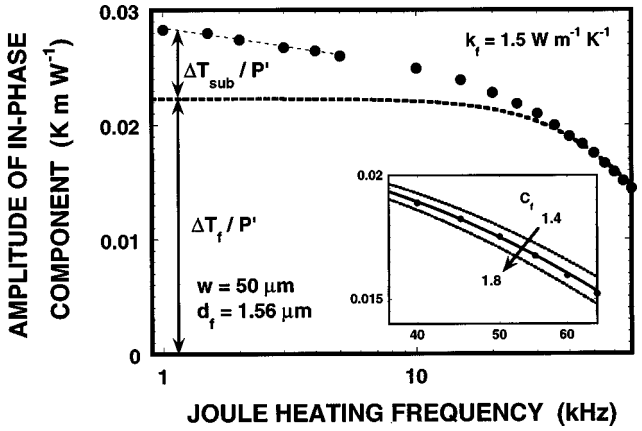

FIG. 3. Frequency dependence of the amplitude of the in-phase component of temperature oscillations in the metal line for the case of the thermally-grown silicon-dioxide layer. The inset is a close-up view of the high-frequency region. Three predictions obtained from the heat diffusion equation are also plotted, which use different values for the film heat capacity.

III. EXPERIMENTAL RESULTS

A. Thermal conductivity of the silicon-dioxide films

Figure 4 shows the measured thermal conductivities of the LPCVD and thermal silicon-dioxide films. The thicknesses of the LPCVD films are around 2 μm and that of the thermal oxide is 1.2 μm. The width of the metal bridge, which serves both as the heater and thermometer, is 50 μm. This value is chosen to be much greater than the dielectric film thickness. This is intended to diminish the impact of lateral heat spreading within the silicon-dioxide films and thereby removes complications arising from possible anisotropy (see Fig. 5).

Thermal resistance at the film interfaces is estimated by repeating measurements on thinner films with thickness down to 100 nm. Under the assumption that the intrinsic film thermal conductivity does not vary appreciably with thickness, an estimate of the thermal boundary resistance can be obtained by extrapolating the total thermal resistance to zero film thickness.[2] The largest estimated boundary resistance value of 2×10^{-8} m^2 K W^{-1} is close to the values reported in the literature[7,8] and results in less than 2% error in the thermal conductivity.

The thermal conductivities of the as-deposited films are more than 30% less than that of the thermally-grown silicon-dioxide film. The difference is diminished appreciably after a high temperature anneal, which is in agreement with a previous study on the annealing temperature dependence of the

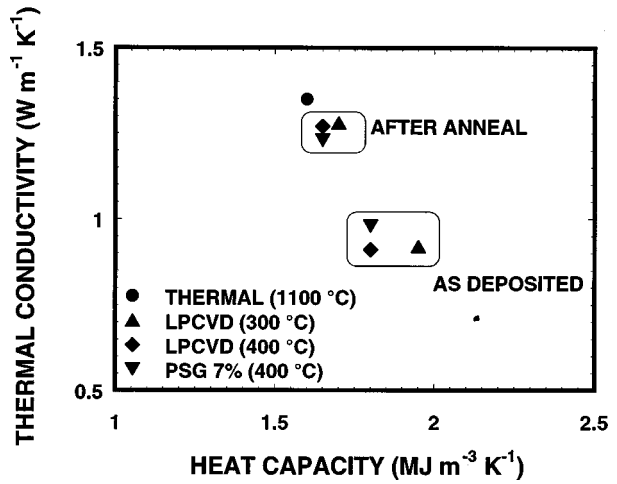

FIG. 4. Thermal conductivities and volumetric heat capacities of the silicon-dioxide films that have experienced different processing histories.

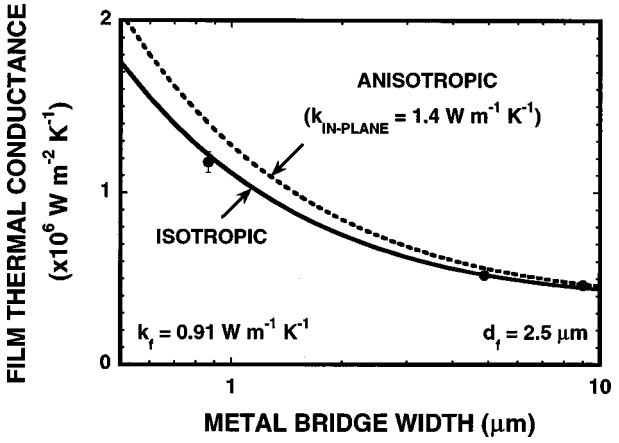

FIG. 5. Predicted and measured thermal conductance of the 2.5 μm-thick LPCVD silicon-dioxide film as a function of the width of the metal bridge structure. In the prediction two different values are used for the in-plane thermal conductivity while the out-of-plane value is fixed at 0.91 $W\,m^{-1}\,K^{-1}$ for both calculations.

thermal conductivity of LPCVD films.[8] Phosphorus and hydrogen impurities have an insignificant effect on the thermal conductivity of the silicon-dioxide films studied here. This can be seen from the fact that the thermal conductivities of the as-deposited films are close to each other despite variations in the concentration of hydrogen atoms in the films (Fig. 6). The annealed films have similar thermal conductivities irrespective of the concentration of phosphorus impurities.

According to the RBS analysis, the densities of the films investigated here do not differ by more than 5%. The observed reduction in the out-of-plane thermal conductivity cannot be explained by the effective medium theory when the density deficit is modeled using spherical microvoids. Highly oriented microvoids, however, can give rise to a pronounced reduction in the out-of-plane conductivity while leaving the in-plane conductivity almost unchanged. This hypothesis is tested using a technique that has been developed to determine the anisotropic thermal conductivity of thin films.[14] The technique employs metal bridges with different widths to induce varying degree of heat spreading within the film. Compared with methods that require free-standing membrane or beam structures, the present method has the advantage of minimizing the possible influence of demanding fabrication steps, such as substrate back etching, on the film properties. Figure 5 shows the film thermal conductance as a function of metal bridge width. Predictions of the heat diffusion equation using two different values for the in-plane thermal conductivity are included for comparison. The data obtained from the LPCVD film indicate that the anisotropy is negligible. Highly oriented microvoids can therefore be ruled out as a possible explanation of the observed thermal conductivity reduction.

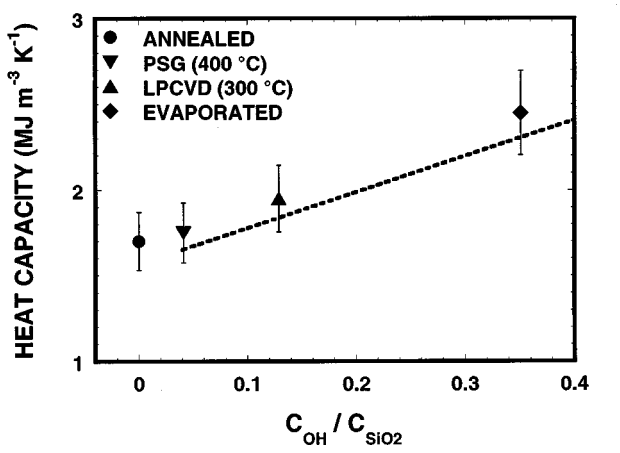

FIG. 6. Measured heat capacities of the LPCVD silicon-dioxide films investigated here as a function of OH bond concentration. The dotted line represents the heat capacity predicted by treating each OH bond as contributing half the heat capacity of a water molecule.

B. Volumetric heat capacity of the silicon-dioxide films

Figure 4 shows the volumetric heat capacities of the silicon-dioxide films. The as-deposited LPCVD silicon-dioxide films have slightly greater heat capacities than that of the thermally-grown silicon-dioxide film. This is rather surprising because the LPCVD films have density deficit near 5%, which is expected to result in corresponding decrease in the volumetric heat capacity. A high-temperature anneal is found to reduce the heat capacity, a trend opposite to what is observed for the thermal conductivity. The presence of an appreciable amount of water, hydroxyl ions and other chemical bonds foreign to silicon dioxide is suspected to be a possible origin of the anomaly. The FTIR spectra of the films are analyzed to determine what fraction of hydrogen atoms are present as silanol and water. The volumetric heat capacity of water is more than 2.5 times larger than that of silicon dioxide at room temperature. Using absorption cross sections reported in the literature for various hydrogen-containing species[16] we find that water and silanol account for more than 85% of the hydrogen atoms in the films. The concentrations of each species are similar to those observed in atmospheric pressure chemical vapor deposition silicon-dioxide films.[17]

Figure 6 plots the heat capacities of the films as a function of OH bond concentration, which is extracted using the FTIR and RBS/HFS analyses. For the annealed LPCVD films, whose FTIR spectra exhibit no detectable absorption peaks associated with hydrogen-related bands, the volumetric heat capacities are comparable to that of the thermally-grown silicon-dioxide film. At an opposite extreme is an evaporated silicon-dioxide film, which contains hydrogen atoms at a concentration of 10 at. %. Since the film is prepared using e-beam evaporation, it is not likely that a significant amount of hydrogen atoms are incorporated during the film deposition process. The hydrogen atoms may be associated with water molecules absorbed when the film is exposed to wet etching and cleaning chemicals and to ambient moisture. During the deposition of the evaporated films the substrate temperature is maintained at 350 K, which yields a film porosity near 10%.

Shown as a dotted line in Fig. 6 is the predicted heat capacity, which is in reasonable agreement with the data.

The heat capacity contribution of each OH bond is assumed to be equivalent to half the heat capacity of a water molecule. The volumetric heat capacity of the *dry* silicon-dioxide film is taken to be that of fused silica with 7% porosity. The actual porosity of the films varies, around 5% for the unannealed LPCVD films and 9.1% for the evaporated film. In contrast to the thermal conductivity, the excess heat capacity correlates reasonably well with the OH bond concentration.

IV. DISCUSSION

The experimental data indicate that the observed thermal conductivity variations cannot be fully accounted for by the consideration of preferentially oriented microvoids, impurities, and process-dependent heat capacity. An alternative proposition is made here, which considers the degree of structural disorder as a major factor influencing the thermal conductivity of amorphous solids. Structural relaxation of vibrational excitations would strongly influence the thermal conductivity without affecting the volumetric heat capacity appreciably.

Previous structural analyses on CVD silicon-dioxide films[18] showed that the average configuration of an SiO_4 tetrahedron, a building block of a continuous random network comprising amorphous silicon dioxide, remains largely unaffected by low-temperature deposition process. In contrast, the root-mean-square deviations in the inter-atomic distances and bond angles, which can serve as one measure of the structural disorder, were found to be considerably larger for as-deposited films than for high-temperature annealed films.[18] These types of structural disorder are expected to most significantly affect the relaxation of vibrational excitations with wavelengths comparable to the bond lengths, a few angstroms in the case of silicon dioxide. The minimum thermal conductivity model[19] indicated that the effective mean free path of heat carriers is of the order of interatomic separations in amorphous materials.

At temperatures above the thermal-conductivity plateau region,[20,21] various heat conduction mechanisms have been proposed to be active in addition to that associated with the propagating modes. Some studies[22] considered hopping of localized vibrational excitations, which occurs via anharmonic interactions with phonons. Structural disorder can affect the frequency range of the localized excitations, as well as their interactions with phonons. Other studies[23–25] focused on heat conduction associated with diffusive as opposed to localized vibrational excitations. These studies also established connection between the structural disorder and thermal conductivity by computing diffusivities of atomic vibrations in model structures with differing degree of disorder. A generalized Einstein model[26,27] considered the random walk of thermal energy between localized oscillators, a mechanism that may be regarded as equivalent to diffusive transport.

V. SUMMARY AND CONCLUSION

The thermal conductivity and volumetric heat capacity of silicon-dioxide films prepared using thermal oxidation and LPCVD are measured. The thermal conductivity of the LPCVD films is reduced from that of thermally-grown silicon dioxide whereas no corresponding decrease is observed for the volumetric heat capacity. The reduction in the thermal conductivity cannot be attributed to anisotropy induced by highly oriented microvoids. The presence of impurities is shown to affect the volumetric heat capacity but not the thermal conductivity. The present experimental data, in conjunction with existing structural analyses on CVD films, strongly suggest that process-dependent structural disorder affects the thermal conductivity of silicon-dioxide films. This conclusion is consistent with previous theoretical studies, which investigated the relation between amount of disorder and thermal conductivity in model amorphous structures.

[1] A. H. Guenther and J. K. Mciver, Thin Solid Films **163**, 203 (1988).
[2] J. C. Lambropoulos, M. R. Jolly, C. A. Amsden, S. E. Gilman, M. J. Sinicropi, D. Diakomihalis, and S. D. Jacobs, J. Appl. Phys. **66**, 4230 (1989).
[3] Y. S. Ju and K. E. Goodson, IEEE Electron Device Lett. **18**, 512 (1997).
[4] D. G. Cahill, M. Katiyar, and J. R. Abelson, Phys. Rev. B **50**, 6077 (1994).
[5] D. G. Cahill and T. H. Allen, Appl. Phys. Lett. **65**, 309 (1994).
[6] S.-M. Lee and D. G. Cahill, Phys. Rev. B **52**, 253 (1995).
[7] S.-M. Lee and D. G. Cahill, J. Appl. Phys. **81**, 2590 (1997).
[8] K. E. Goodson, M. I. Flik, L. T. Su, and D. A. Antoniadis, IEEE Electron Device Lett. **14**, 490 (1993).
[9] M. B. Kleiner, S. A. Kühn, and W. Weber, IEEE Trans. Electron Devices **43**, 1602 (1996).
[10] R. Landauer, J. Appl. Phys. **23**, 779 (1952).
[11] D. G. Cahill, R. H. Tait, R. B. Stephens, S. K. Watson, and R. O. Pohl, in *Thermal Conductivity*, edited by C. J. Cremers and H. A. Fine (Plenum, New York, 1990), Vol. 21, pp. 3–16.
[12] C. J. Morath, H. J. Maris, J. J. Cuomo, D. L. Pappa, A. Grill, V. V. Patel, J. P. Doyle, and K. L. Saenger, J. Appl. Phys. **76**, 2636 (1994).
[13] D. G. Cahill, Rev. Sci. Instrum. **61**, 802 (1990).
[14] Y. S. Ju, K. Kurabayashi, and K. E. Goodson, Thin Solid Films **339**, 160 (1999).
[15] M. Okuda and S. Ohkubo, Thin Solid Films **213**, 176 (1992).
[16] A. C. Adams, Solid State Technol. **26**, 135 (1983).
[17] S. Rojas, L. Zanotti, A. Borghesi, A. Sassella, and G. U. Pignatel, J. Vac. Sci. Technol. B **11**, 2081 (1993).
[18] N. Nagasima, J. Appl. Phys. **43**, 3378 (1972).
[19] C. Kittel, Phys. Rev. **75**, 972 (1949).
[20] R. C. Zeller and R. O. Pohl, Phys. Rev. B **4**, 2029 (1971).
[21] J. J. Freeman and A. C. Anderson, Phys. Rev. B **34**, 5684 (1986).
[22] A. Jagannathan, R. Orbach, and O. Entin-Wohlman, Phys. Rev. B **39**, 13 465 (1989).
[23] P. B. Allen and J. L. Feldman, Phys. Rev. B **48**, 12 581 (1993).
[24] J. L. Feldman, M. D. Kluge, P. B. Allen, and F. Wooten, Phys. Rev. B **48**, 12 589 (1993).
[25] P. Sheng and M. Zhou, Science **253**, 539 (1991).
[26] D. G. Cahill and R. O. Pohl, Solid State Commun. **70**, 927 (1989).
[27] D. G. Cahill, S. K. Watson, and R. O. Pohl, Phys. Rev. B **46**, 6131 (1992).
[28] M.-A. Einarsrud, S. Haereid, and V. Wittwer, Sol. Energy Mater. Sol. Cells **31**, 341 (1993).